Removal of Arbitrary Discontinuities in Atmospheric Density Modeling*

Sergei Tanygin   James R. Wright

Analytical Graphics, Inc.

February 2, 2004

Abstract

The use of discontinuous a_P values, for the simultaneous sequential estimation of six spacecraft LEO parameters, atmospheric density, ballistic coefficient, and other observable paramters, results in the failure of McReynolds' Filter-Smoother Consistency Test. But this test is satisfied when input values of a_P are splined (smoothed) before use. The three-hourly discontinuities in a_P are always wrong in the sense that three-hourly discontinuities are never produced by the magnetometers from which a_P is derived. Our purpose herein is two-fold: (i) Present graphical results for McReynolds' Filter-Smoother Consistency Tests (ii) Record and present the development of the osculating polynomial splines we have used to smooth the discontinuous a_P function.

1 Introduction

For the sequential orbit determination of a spacecraft in LEO from real range tracking data, we have demonstrated the satisfaction[12] of McReynolds' Filter-Smoother Consistency Test, in spacecraft position, when input values of a_P are splined (smoothed) before use. Also, with the same real data, we have demonstrated failure of the Filter-Smoother Consistency Test when the 3-hourly step functions in a_P are used. These contrasting results are presented graphically.

The development of osculating polynomial splines used to smooth the discontinuous step functions in a_P is presented. This invokes the development of polynomial basis functions, and the application of a least squares (LS) algorithm to solve the underdetermined LS problem. The latter is compared to the widely used overdetermined LS algorithm via the definition for generalized-inverse (pseudo-inverse). The actual underdetermined LS solution is calculated with an orthogonal decompostion of a LS rectangular matrix relating solution to given a_P data.

2 McReynolds' Filter-Smoother Consistency Test

2.1 Filter-Smoother Description

Real range tracking data measurements were processed by a sequential filter[1] to estimate a 22 parameter state. The state estimate, for the computer runs and graphics referred to herein, contained 6 parameters for spacecraft LEO position and velocity, 1 parameter for relative atmospheric density, 1 parameter for relative spacecraft ballistic coefficient, and 14 parameters for range biases; i.e., 1 parameter for each of 14 AFSCN ground station radar sensors.

The filter does input and process measurement data sequentially forward with time, and responds with a complete state estimate and error covariance within milli-seconds[2] of receipt of each measurement. This is enabled by accumulation of information from the infinite past, and by satisfaction of the requirements for optimal orbit determination[3][13]. The real-time filtered state estimate and covariance are used as initial conditions for their forward propagation.

The smoother does input and process stored filter data sequentially backward with time, using the last filter state estimate and error covariance matrix, and associated epoch t_L as initial conditions. With decreasing time, the smoother input is defined by stored filter output together with recursively generated smoother output. Measurements are not reprocessed by the smoother. The smoothed state estimate is superior to the filtered state estimate for each time $t_k < t_L$.

---

*© Analytical Graphics, Inc., 2004. Paper AAS 04-176 published by AAS/AIAA with permission.

[1] The sequential filter and smoother are algorithms embedded in software for STK/OD, a product of Analytical Graphics, Inc.

[2] This has been demonstrated on a PC.

[3] This paper can be viewed on line at: http://www.stk.com/resources. Under *Documentation* click *White Papers*.

2.2 Filter-Smoother Consistency Test

For each parameter of the state, a unitless ratio is formed. The ratio numerator consists of the difference between filtered and smoothed state estimate at a common time. The ratio denominator consists of a root-variance (sigma) on the numerator difference, derived from the filtered and smoothed state estimate error covariance function. Each state parameter ratio can be graphed as a function of time. McReynolds' Filter-Smoother Consistency Test consists in comparing this unitless ratio to ± 3. If 99% of the ratios graphed fall between -3 and 3, then the test is defined a success[4]. If not, the test is defined a failure.

Initialization of the sequential filter requires the processing of measurement data across the filter initialization time interval. Since initialization is required to develop realistic covariance elements, the Filter-Smoother Consistency Test is ignored during filter initialization.

Figs. 4 and 5 present failure and success, of McReynolds' Filter-Smoother Consistency Test, in three components of spacecraft position. The *failure* responds to the use of discontinuous a_P step functions for atmospheric density model inputs. The *success* responds to the use of smooth a_P cubic splines for atmospheric density model inputs.

3 The Discontinuous a_P Function

We are given m values of the geomagnetic index $a_P(\tau_i, \tau_{i+1})$, $i \in \{0, 1, 2, \ldots, m-1\}$, where:

- $\tau_i \in \{0_d^h, 3_d^h, 6_d^h, \ldots, 21_d^h\}$ UTC for each day d of the year

- $a_P(\tau_i, \tau_{i+1})$ is a time constant across each interval $[\tau_i, \tau_{i+1}]$

- $\tau_{i+1} - \tau_i = 3$ hours

- $a_P(\tau_i, \tau_{i+1})$ may be (is usually) discontinuous at each 3 hour partition knot-point τ_i, $i \in \{0, 1, 2, \ldots, m-1\}$

Capture the given data in an $m \times 1$ matrix b:

$$b = \begin{bmatrix} a_P(\tau_0, \tau_1) \\ a_P(\tau_1, \tau_2) \\ \vdots \\ a_P(\tau_{m-1}, \tau_m) \end{bmatrix} \tag{1}$$

Then matrix b presents a discontinuous function $g_{a_P}(\tau)$, $\tau_0 \leq \tau \leq \tau_m$. But the elements of b are derived from magnetometer measurements that are continuous with time. We wish to construct a function $g(\tau)$ that:

- Approximates $a_P(\tau_i, \tau_{i+1})$, for all $i \in \{0, 1, 2, \ldots, m-1\}$

- Is continuous and smooth (differentiable) at each partition time point τ_i and at all other times $\tau \in [\tau_0, \tau_m]$

- Satisfies the integral constraint:

$$\int_{\tau_i}^{\tau_{i+1}} g(\tau) \, d\tau = [\tau_{i+1} - \tau_i] \, a_P(\tau_i, \tau_{i+1}), \, i \in \{0, 1, 2, \ldots, m-1\} \tag{2}$$

Function $g(\tau)$ will be composed of a sequence of polynomial splines, connected at interior *knot-point* times τ_i, $i \in \{1, 2, \ldots, m-1\}$.

---

[4]The bases for this test consist of the use of the Normal density function for state estimation error modeling, extensive experience with comparisons of error modeling with the Normal density function, and the Central Limit Theorem.

4 Osculating Polynomial Splines

It will prove convenient to define a constant T and time transformation $t(\tau)$ with:

$$T = \tau_{i+1} - \tau_i \tag{3}$$

$$t(\tau) = \tau - \tau_i \tag{4}$$

so that:

$$t(\tau_i) = 0 \tag{5}$$

$$t(\tau_{i+1}) = T \tag{6}$$

$$0 \le t \le T \tag{7}$$

The inverse transformation $\tau(t)$ derives from Eq. 4:

$$\tau(t) = t + \tau_i \tag{8}$$

$$\tau(0) = \tau_i \tag{9}$$

$$\tau(T) = \tau_{i+1} \tag{10}$$

Adopt the shorthand notation $a_P = a_P(0, T)$ when referring to time t, and $a_P^{i,i+1} = a_P(\tau_i, \tau_{i+1})$ when referring to UTC time τ. Denote $g(\tau(t))$, a function of t, with the name $f(t)$:

$$f(t) = g(\tau(t)) \tag{11}$$

Function $f(t)$ is defined by Eq. 17. With the aid of Eq. 3, Eq. 2 can be written:

$$F = \int_0^T f(t)\,dt = T a_P \tag{12}$$

where F denotes a definite integral of $f(t)$.

4.1 Third-Order Polynomial Structures

We are interested in the use of third-order polynomials $p(t)$ and $r(t)$:

$$p(t) = a_0 + a_1 t + a_2 t^2 + a_3 t^3 \tag{13}$$

$$r(t) = b_0 + b_1 t + b_2 t^2 + b_3 t^3 \tag{14}$$

Differentiate them with time:

$$\dot{p}(t) = a_1 + 2a_2 t + 3a_3 t^2 \tag{15}$$

$$\dot{r}(t) = b_1 + 2b_2 t^1 + 3b_3 t^2 \tag{16}$$

These four polynomials provide the structure to develop a basis[1] for $f(t)$. By *basis* we refer to a set of polynomials that are independent, and are defined such that any realization of $f(t)$ can be expressed as a linear combination of them.

4.2 Two-Point Osculating Splines

Define $f(t)$ with:

$$f(t) = f_0 p_0(t) + \dot{f}_0 r_0(t) + f_T p_T(t) + \dot{f}_T r_T(t) \tag{17}$$

Eq. 17 is the key to two-point osculating splines. Differentiate Eq. 17 to get:

$$\dot{f}(t) = f_0 \dot{p}_0(t) + \dot{f}_0 \dot{r}_0(t) + f_T \dot{p}_T(t) + \dot{f}_T \dot{r}_T(t) \tag{18}$$

For each time interval $[0, T]_t = [\tau_i, \tau_{i+1}]_\tau$, require that:

$$f_0 = f(0) = g(\tau_i) \tag{19}$$

$$f_T = f(T) = g(\tau_{i+1}) \tag{20}$$

$$\dot{f}_0 = \dot{f}(0) = \dot{g}(\tau_i) \tag{21}$$

$$\dot{f}_T = \dot{f}(T) = \dot{g}(\tau_{i+1}) \tag{22}$$

4.3 Derive Osculating Basis Polynomials

Evaluate Eqs. 17 and 18 at $t = 0$ and $t = T$ to get:

$$p_0(0) = p_T(T) = \dot{r}_0(0) = \dot{r}_T(T) = 1 \tag{23}$$

$$r_0(0) = r_T(0) = r_T(T) = r_0(T) = p_0(T) = p_T(0) = 0 \tag{24}$$

$$\dot{p}_0(0) = \dot{p}_0(T) = \dot{p}_T(0) = \dot{p}_T(T) = \dot{r}_0(T) = \dot{r}_T(0) = 0 \tag{25}$$

Now $p_0(0) = 1$ implies $a_0 = 1$, and $\dot{p}_0(0) = 0$ implies $a_1 = 0$. Insert these evaluations into Eqs. 13 and 15 to get two equations in the two unknowns a_2 and a_3. Then:

$$a_2 = -3/T^2 \tag{26}$$

$$a_3 = 2/T^3 \tag{27}$$

Insert these evaluations into Eq. 13 to derive the osculating basis polynomial:

$$p_0(t) = \left[1 + 2\left(\frac{t}{T}\right)\right]\left[\frac{(t-T)^2}{T^2}\right] \tag{28}$$

In a similar manner, derive:

$$p_T(t) = \left[3 - 2\left(\frac{t}{T}\right)\right]\left[\frac{t^2}{T^2}\right] \tag{29}$$

$$r_0(t) = \frac{t(t-T)^2}{T^2} \tag{30}$$

$$r_T(t) = \frac{(t-T)t^2}{T^2} \tag{31}$$

$$\dot{p}_0(t) = \frac{6t(t-T)}{T^3} \tag{32}$$

$$\dot{p}_T(t) = -\frac{6t(t-T)}{T^3} \tag{33}$$

$$\dot{r}_0(t) = \frac{(t-T)(3t-T)}{T^2} \tag{34}$$

$$\dot{r}_T(t) = \frac{t(3t-2T)}{T^2} \tag{35}$$

From Eqs. 17 and 23, function $f(t)$ is seen to be coincident with basis function $p_0(t)$ at $t=0$, and coincident with basis function $p_T(t)$ at $t=T$. From Eqs. 18 and 23, the derivative function $\dot{f}(t)$ is seen to be coincident with basis function $\dot{r}_0(t)$ at $t=0$, and coincident with basis function $\dot{r}_T(t)$ at $t=T$. These are the two points of osculation[5] (tangency) for $f(t)$. And so function $f(t)$ is coincident with, and tangent to, polynomial basis functions at two time points $t=0$ and $t=T$.

5   Integral Constraints

Insert Eq. 17 into Eq. 12:

$$F = \int_0^T \left[f_0 p_0(t) + \dot{f}_0 r_0(t) + f_T p_T(t) + \dot{f}_T r_T(t) \right] dt$$

$$= f_0 P_0 + \dot{f}_0 R_0 + f_T P_T + \dot{f}_T R_T \tag{36}$$

where:

$$P_0 = \int_0^T p_0(t)\,dt = \frac{T}{2} \tag{37}$$

$$R_0 = \int_0^T r_0(t)\,dt = \frac{T^2}{12} \tag{38}$$

$$P_T = \int_0^T p_T(t)\,dt = \frac{T}{2} \tag{39}$$

$$R_T = \int_0^T r_T(t)\,dt = -\frac{T^2}{12} \tag{40}$$

$$P_T = P_0, \text{ and } R_T = -R_0 \tag{41}$$

Then:

$$F = (f_0 + f_T) P_0 + \left(\dot{f}_0 - \dot{f}_T \right) R_0 = Ta_P \tag{42}$$

or with indexing $i \in \{0, 1, 2, \ldots, m-1\}$:

$$F^{i,i+1} = \left(f_0^{i,i+1} + f_T^{i,i+1} \right) P_0 + \left(\dot{f}_0^{i,i+1} - \dot{f}_T^{i,i+1} \right) R_0 = Ta_P^{i,i+1} \tag{43}$$

where the superscripts identify a particular 3-hour time interval, and the subscripts distinguish interval ends; i.e., $t=0$ begins the interval, and $t=T$ ends the interval. Thus $f_0^{i,i+1}$ is the value of $f(t)$ at the beginning $t=0$ of the time interval spanned by $a_P^{i,i+1}$. The requirement for continuity and smoothness at each interior knot-point means that the following $2(m-1)$ conditions must be satisfied:

$$f_T^{i+1} = f_0^i \tag{44}$$

---

[5] The nonlinear theory of variation of parameters, from celestial mechanics, derives from the requirement that the position and velocity of the two-body conic be coincident with the position and velocity of the perturbed trajectory. The constant orbit elements of the two-body conic are thereby transformed to time-varying orbit elements. The time-varying conic is then referred to as an osculating (kissing) orbit.

$$\dot{f}_T^{i+1} = \dot{f}_0^i \tag{45}$$

Then Eq. 43 becomes:

$$F^{i,i+1} = \left(f_0^{i,i+1} + f_0^{i+1,i+2} \right) P_0 + \left(\dot{f}_0^{i,i+1} - \dot{f}_0^{i+1,i+2} \right) R_0 = T a_P^{i,i+1} \tag{46}$$

for $i \in \{0, 1, 2, \ldots, m-1\}$. Eq. 46 can now be written, without ambiguity as:

$$F^{i,i+1} = \left(f^i + f^{i+1} \right) P_0 + \left(\dot{f}^i - \dot{f}^{i+1} \right) R_0 = T a_P^{i,i+1} \tag{47}$$

for $i \in \{0, 1, 2, \ldots, m-1\}$. We have m equations in $2m+2$ unknowns. Add on zero slope end intervals to nail down end points:

$$a_P^{-1,0} = a_P^{0,1} \text{ and } a_P^{m,m+1} = a_P^{m-1,m} \tag{48}$$

6 Restructure Eq. 47

Refer to the given a_P values $a_P^{i,i+1}$, $i \in \{0, 1, 2, \ldots, m-1\}$, as measurements. To move measurement information onto the time grid t_i, $i \in \{0, 1, 2, \ldots, m\}$, associated with f^i and $\dot{f}^i$, construct psuedo measurements a_P^i:

$$a_P^i = \left(a_P^{i-1,i} + a_P^{i,i+1} \right) / 2 \tag{49}$$

Define $\hat{f}^i$:

$$\hat{f}^i = \left(f^i - a_P^i \right) / T \tag{50}$$

and define:

$$\hat{P}_0 \equiv P_0 T = T^2 / 2 \tag{51}$$

Then for $i \in \{0, 1, 2, \ldots, m-1\}$, Eq. 47 becomes:

$$\left(\hat{f}^i + \hat{f}^{i+1} \right) \hat{P}_0 + \left(\dot{f}^i - \dot{f}^{i+1} \right) R_0 = y^i \tag{52}$$

where:

$$y^i = T a_P^{i,i+1} - \hat{P}_0 \left(a_P^{i-1,i} + 2 a_P^{i,i+1} + a_P^{i+1,i+2} \right) / (2T) \tag{53}$$

If zero slope is desired at the knot-points, then set $\dot{f}^i = \dot{f}^{i+1} = 0$. Refer to this as the *Reduced Least Squares* condition.

7 Least Squares

Our purpose here is to estimate values for f^i and $\dot{f}^i$, $i \in \{0, 1, 2, \ldots, m\}$, from values of $a_P^{i,i+1}$, $i \in \{0, 1, 2, \ldots, m-1\}$, using a least squares algorithm.

7.1 Matrix Definitions

Define an $n \times 1$ matrix x, where $n = 2(m+1)$:

$$x = \left(\hat{f}^0, \dot{f}^0, \hat{f}^1, \dot{f}^1, \ldots, \hat{f}^m, \dot{f}^m \right)^T \tag{54}$$

Define an $m \times 1$ matrix y:

$$y = \left(y^0, y^1, \ldots, y^{m-1} \right)^T \tag{55}$$

Define an $m \times n$ matrix A:

$$A = \begin{bmatrix} \hat{P}_0 & R_0 & \hat{P}_0 & -R_0 & 0 & 0 & 0 & \cdots & 0 & 0 \\ & & \hat{P}_0 & R_0 & \hat{P}_0 & -R_0 & 0 & \cdots & 0 & 0 \\ \cdots & \cdots & \cdots & \cdots & \cdots & \cdots & \cdots & \cdots & \cdots & \cdots \\ 0 & 0 & 0 & 0 & \cdots & 0 & \hat{P}_0 & R_0 & \hat{P}_0 & -R_0 \end{bmatrix} \tag{56}$$

Use Eq. 52 to write a matrix least squares equation[2]:

$$Ax = y \tag{57}$$

where $m < n$.

7.2 Generalized Matrix Inverse

For many least squares problems we have the over-determined relation $m > n$ associated with the least squares normal equation, and this invokes a generalized matrix inverse, call it A^+. It is therefore useful to review all three relations for m and n. So here we seek all solutions x to Eq. 57 that minimize length $\|x - A^+ y\|$, where A is an $m \times n$ matrix with rank m or n, x is an $n \times 1$ matrix, y is an $m \times 1$ matrix, and where $m = n$, or $m < n$, or $m > n$.

7.2.1 $m = n$

When matrix A is square and has rank $m = n$, then calculate the matrix inverse A^{-1} and solve Eq. 57 for $x = A^{-1}y$.

7.2.2 $m \neq n$

But when matrix A is non-square with $m \neq n$, invoke a generalized matrix inverse A^+ such that:

$$x = A^+ y \tag{58}$$

where length $\|x - A^+ y\|$ is minimized. Penrose[2][3] showed that for every real finite matrix A there exists a unique generalized matrix inverse A^+, that satisfies the Penrose conditions:

$$AA^+A = A \tag{59}$$

$$A^+AA^+ = A^+ \tag{60}$$

$$\left(AA^+\right)^T = AA^+ \tag{61}$$

$$\left(A^+A\right)^T = A^+A \tag{62}$$

Now $\left(A^T A\right)$ is an $n \times n$ matrix and $\left(AA^T\right)$ is an $m \times m$ matrix. If $\text{Rank}(A) = n$, then $\text{Rank}\left(A^T A\right) = n$ and $\left(A^T A\right)$ can be inverted. If $\text{Rank}(A) = m$, then $\text{Rank}\left(AA^T\right) = m$ and $\left(AA^T\right)$ can be inverted. Adopt the following generalized inverse definitions[6]: If $\text{Rank}(A) = n$, define:

$$A^+ = A_n^+ = \left(A^T A\right)^{-1} A^T \tag{63}$$

If $\text{Rank}(A) = m$, define:

$$A^+ = A_m^+ = A^T \left(AA^T\right)^{-1} \tag{64}$$

Both A_n^+ and A_m^+ are generalized inverse matrices because they satisfy the four Penrose conditions. Insert Eq. 63 into Eq. 58 to get the classical normal equation solution for overdetermined least squares problems. Insert Eq. 64 into Eq. 58 to get the classical solution for underdetermined least squares problems.

---

[6] Lawson and Hanson[2], Excersize 7.24.

7.2.3 Formal Solution

For our osculating polynomials, $m < n$, and $\mathrm{Rank}(A) = m$. Then insert Eq. 64 into Eq. 58 to get:

$$x = A_m^+ y = A^T \left(AA^T\right)^{-1} y \tag{65}$$

Eq. 65 could be used to evaluate our polynomial coefficients, but there is a more efficient and numerically accurate solution.

7.3 Efficient and Accurate Solution

Perform the orthogonal decomposition[2]:

$$A = HRK^T \tag{66}$$

where H is an $m \times m$ orthogonal matrix, K is an $n \times n$ orthogonal matrix, and R is an $m \times n$ matrix:

$$R = \left[\ \begin{matrix} R_{11} & 0 \end{matrix}\ \right] \tag{67}$$

where R_{11} is a non-singular triangular $m \times m$ matrix of rank m. The non-zero singular values of A, R and R_{11} appear on the diagonal of triangular matrix R_{11}. Since H and K are orthogonal:

$$R = H^T A K \tag{68}$$

A generalized inverse matrix R^+ to R is defined by:

$$R^+ = \left[\ \begin{matrix} R_{11}^{-1} & 0 \end{matrix}\ \right] \tag{69}$$

Then the unique, and most simple[7], efficient, and numerically accurate, least squares solution x to Eq. 57, where length $\|x - A^+ y\|$ is minimized, is given by:

$$x = KR^+ H^T y \tag{70}$$

The coefficients for our osculating polynomials can be calculated, by back substitutions, from the n elements of x.

8 Graphics

8.1 Arbitrary Examples of Osculating Cubic Splines

Arbitrary examples of integral preserving cubic spline sequences are displayed in Figs. 1, 2, and 3. Each spline is overlaid on the square-wave graph to which it is fit. The square-wave graph consists of a discontinuous sequence of constant bars with each bar of unit length, parallel to the x axis. Recall that $[0, T]$ is the time interval, and T is the time length, of each osculating polynomial spline. Fig. 1 presents $1T/bar$, Fig. 2 presents $2T/bar$, and Fig. 3 presents an overlay with $1T/bar$, $2T/bar$, and $10T/bar$. As n grows, for nT/bar, the spline sequence approximates the original square-wave graph more closely. Thus the integral preserving $1T/bar$ sequence is fartherest from the square-wave graph. The $1T/bar$ sequence was used to smooth the a_P values referred to here in the simultaneous estimation of a LEO, together with atmospheric density[12] ballistic coefficient, and other observable state parameters.

The *Reduced LS* curve, overlaid on Figs. 1 and 2, refers to the *Reduced Least Squares* condition defined above.

8.2 McReynolds' Filter-Smoother Consistency Tests

8.2.1 Filter-Smoother Test Description

Figs. 4 and 5 present failure and success, of McReynolds' Filter-Smoother Consistency Test, in three components of spacecraft position. The *failure* responds to the use of discontinuous a_P step functions for atmospheric density model inputs. The *success* responds to the use of smooth a_P cubic splines for atmospheric density model inputs.

---

[7] One can also obtain an equivalent least squares solution with singular value decomposition (SVD). But SVD is not quite so simple.

References

[1] Davis, Philip J., *Interpolation and Approximation*, Dover Pub., New York, 1963, 1975

[2] Lawson, Charles L., *Solving Least Squares Problems*, Prentice-Hall, Englewood Cliffs, New Jersey, 1974

[3] Ben-Israel, Adi, Greville, Thomas N. E., *Generalized Inverses, Theory and Applications*, John Wiley, New York, 1974

[4] Golub, Gene H., Van Loan, Charles F., *Matrix Computations*, John Hopkins UnuvMeeting, Ponce, Puerto Rico, 9-13 February, 2003

[5] L. G. Jacchia, *Revised Static Models of the Thermosphere and Exosphere with Empirical Temperature Profiles*, Smithsonian Astrophysical Observatory, Special Report 332, 1971

[6] Sherman, S., *A Theorem on Convex Sets with Applications*, Ann. Math. Stat., 26, 763-767, 1955.

[7] Sherman, S., *Non-Mean-Square Error Criteria*, IRE Transactions on Information Theory, Vol. IT-4, 1958.

[8] Kalman, R. E., *New Methods in Wiener Filtering Theory,* Proceedings of the First Symposium on Engineering Applications of Random Function Theory and Probability, edited by J. L. Bogdanoff and F. Kozin, John Wiley & Sons, New York, 1963.

[9] Rauch, H. E., *Solutions to the Linear Smoothing Problem*, IEEE Trans.Autom. Control, vol. AC-8, p. 371, 1963

[10] Meditch, J. S., *Stochastic Optimal Linear Estimation and Control*, McGraw-Hill, New York, 1969.

[11] James R. Wright, *Real-Time Estimation of Local Atmospheric Density*, Paper AAS 03-164, 13th AAS/AIAA Space Flight Mechanics Meeting, Ponce, Puerto Rico, 9-13 February 2003.

[12] James R. Wright, James Woodburn, *Simultaneous Real-Time Estimation of Atmospheric Density and Ballistic Coefficient*, 14th AAS/AIAA Space Flight Mechanics Conference, Maui, Hawaii, 8-12 February 2004.

[13] James R. Wright, *Optimal Orbit Determination*, Paper AAS 02-192, AAS/AIAA Space Flight Mechanics Meeting, San Antonio, Texas, 27-30 Jan., 2002.

[14] Chris Sabol, K. Kim Luu, *Atmospheric Density Dynamics and the Motion of Satellites*, Air Force Research Laboratory, Directed Energy Directorate, 535 Lipoa Parkway, Suite 200, Kihei, HI 96753, Paper given: 2002 AMOS Technical Conference, Wailea, HI, Sept. 2002
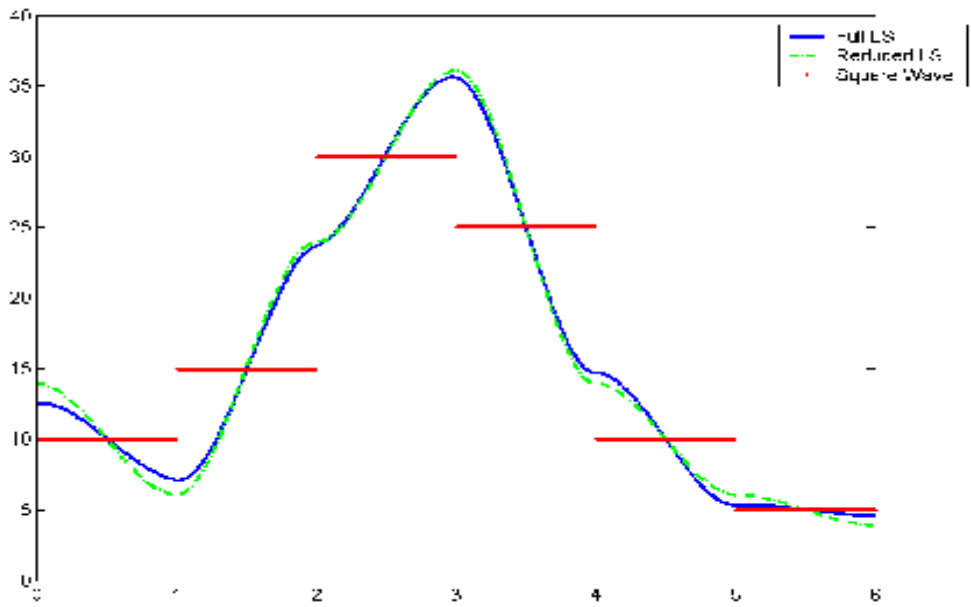
Figure 1: Integral Preserving Cubic Spline, $1T/bar$
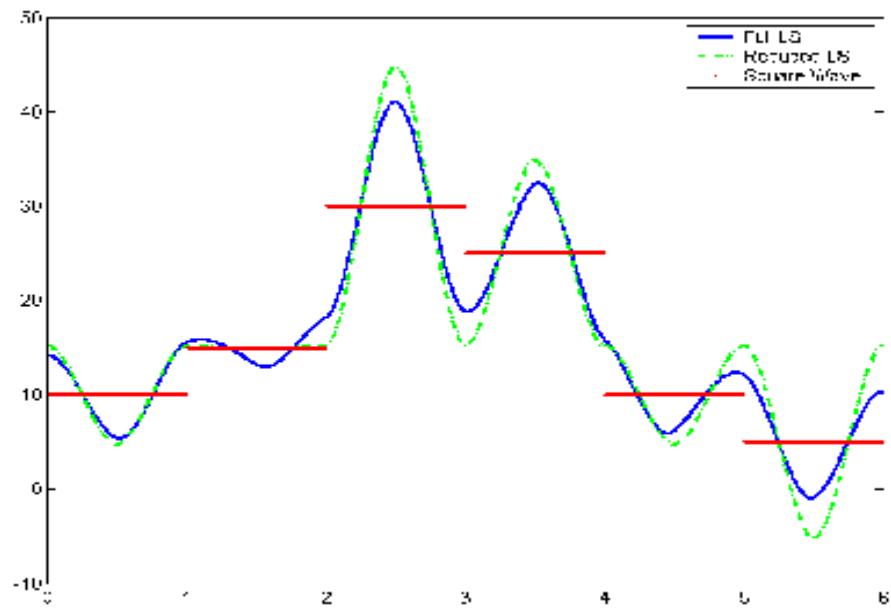
Figure 2: Integral Preserving Cubic Spline, $2T/bar$
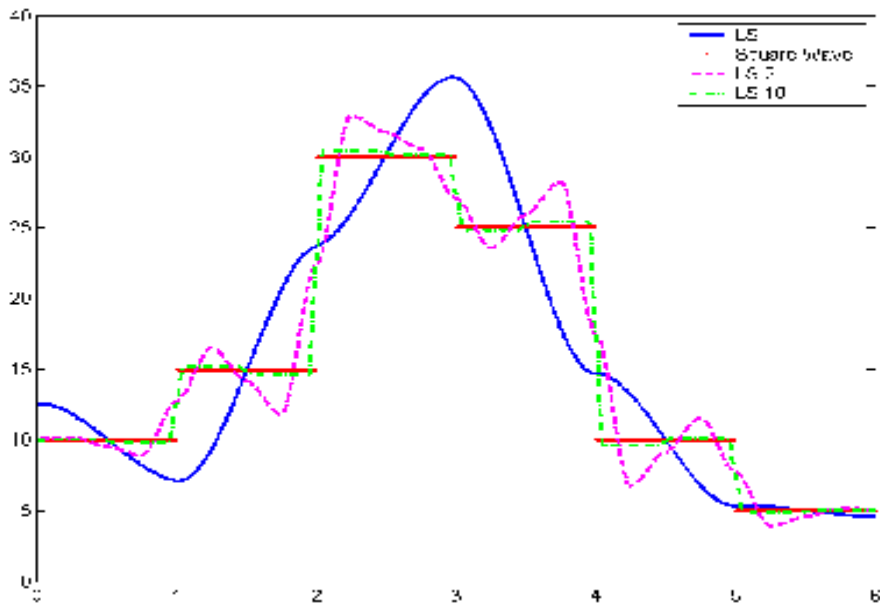
Figure 3: Integral Preserving Cubic Spline, $1T/bar$, $2T/bar$, $10T/bar$
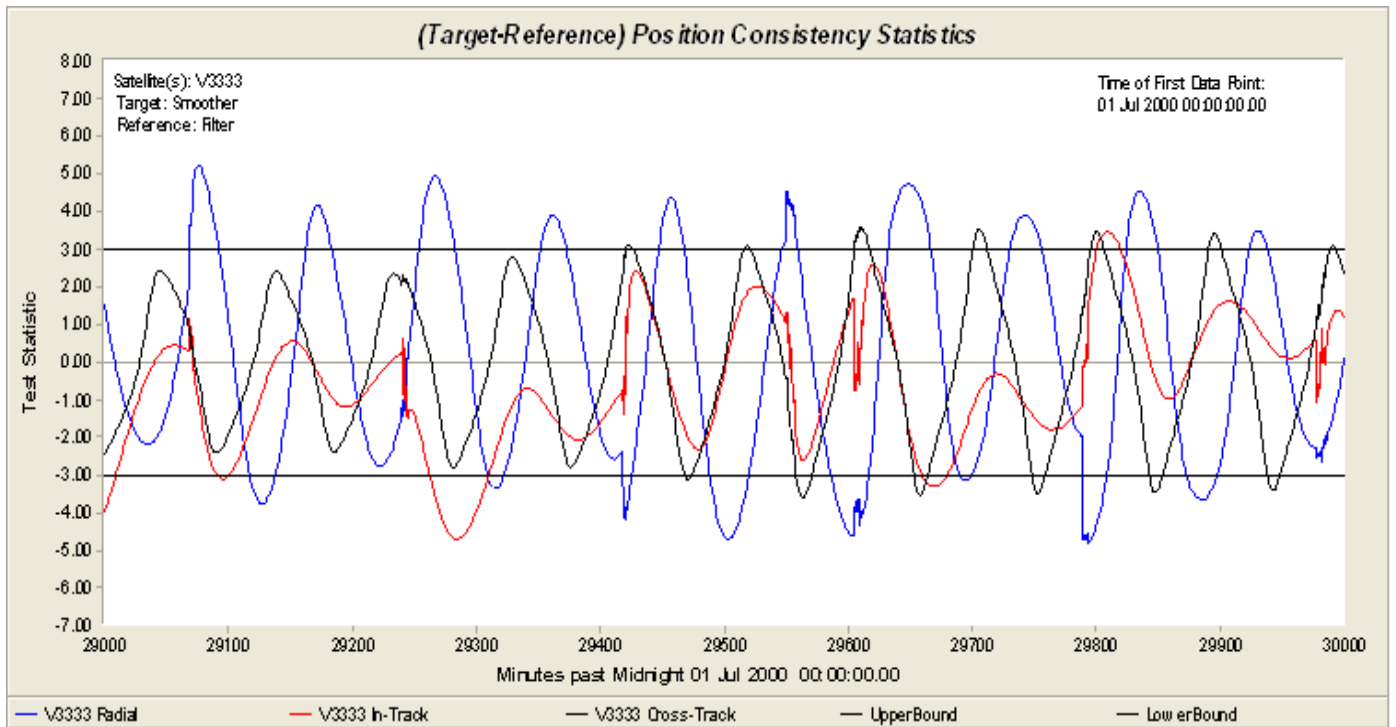
Figure 4: Failure of Filter-Smoother Test using Discontinuous a_P 3-Hourly Step Function
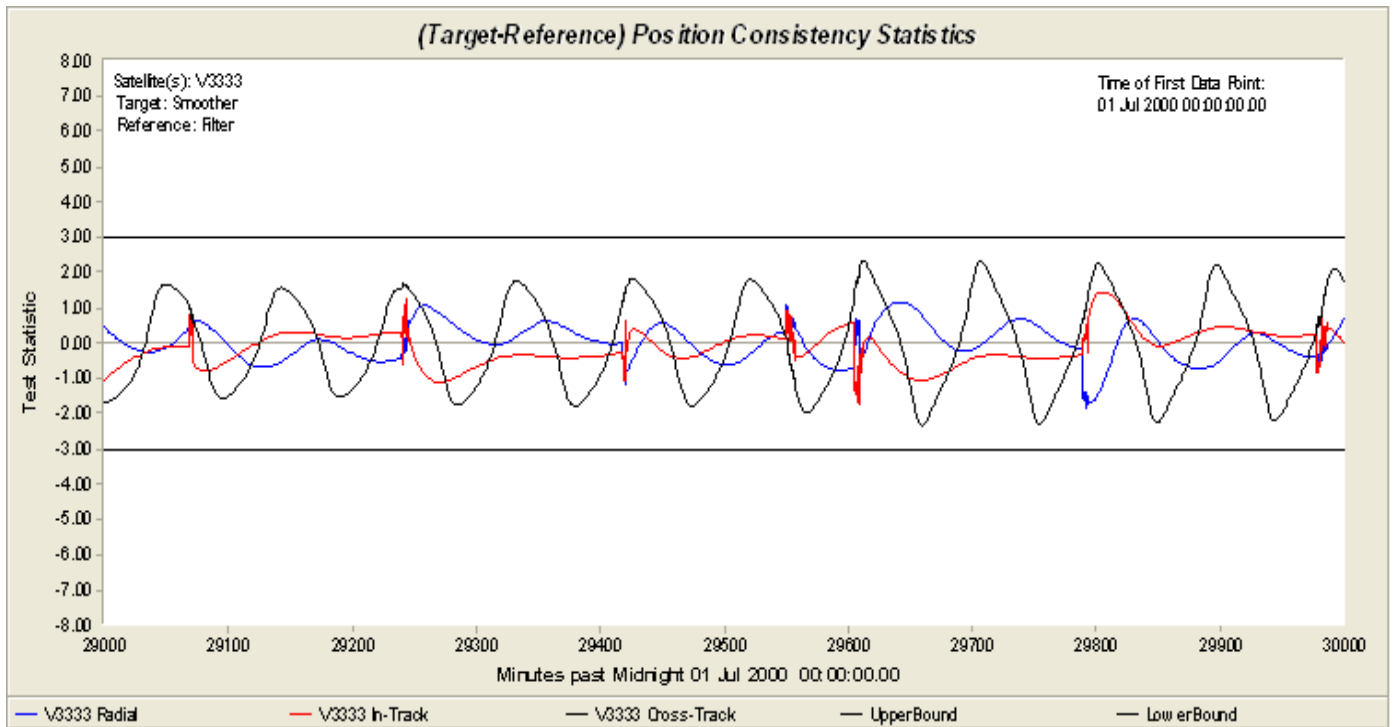
Figure 5: Success of Filter-Smoother Test with a_P Osculating Spline Function